

ATMOSPHERIC PROFILES FROM RADIO OCCULTATION MEASUREMENTS OF GPS SATELLITES

E. Robert Kursinski and George A. Hajj
California Institute of Technology
Jet Propulsion Laboratory
Pasadena, CA 91109

Kenneth R. Hardy
Lockheed Missiles and Space Company, Inc.,
0/91 -20 B/255
3251 Hanover St., Palo Alto, CA 94304-1191

ABSTRACT

Atmospheric profiles can be retrieved with techniques utilizing measurements of the propagation delay of signals from Global Positioning System (GPS) satellites observed by one or more receivers in low earth orbit. The observations are made in a limb-sounding geometry when the radio path between the transmitter and receiver passes through the atmosphere. The various components of the microwave refractivity of the earth's atmosphere are described and in particular the effect of liquid water suspended in the atmosphere is examined. We briefly describe the retrieval technique and the information it provides. We then discuss the impulse response of the retrieval technique and provide an intuitive description of the effect of horizontal structure on the retrieval process. We conclude with examples of the ability to separate temperature and water vapor densities in measurements made in the lower troposphere.

1. INTRODUCTION

Profiles of atmospheric refractivity can be retrieved with techniques utilizing measurements of the propagation delay of signals from Global Positioning System (GPS) satellites observed by one or more receivers in low earth orbit (LEO). This is an application of the radio occultation technique which has a heritage of more than 25 years in NASA's planetary science program. The radio signal propagating from the GPS transmitter to the LEO receiver follows a path through the terrestrial atmosphere that curves distinctively in response to gradients in atmospheric refractive index. The slowing of the signal as it travels along the curved path produces an extra optical length in addition to the direct path traveled in the absence of the atmosphere.

The cumulative effect of the atmosphere on the ray path can be expressed in terms of the total refractive bending angle, a , as a function of the impact parameter, a . The impact parameter is defined as the perpendicular distance between the center of the local curvature near the tangent point of the ray and the asymptotic straight line followed by the ray as it approaches the atmosphere (Fig. 1). For an atmosphere with local spherical symmetry (i. e., no horizontal variations in refractive index), there is a unique relationship between $\alpha(a)$ and $p(r)$, the atmospheric refractive index as a function of radius r . Specifically, $p(r)$ is obtained through integration of $\alpha(a)$, where the integral is a specific case of the Abel transform. In the more general case where the contours of constant refractivity are oblate in response to the non-spherical gravity field of a planet, the nonspherical inversion can be performed*. In the most general case, raytracing can be used in the inversion process,

The fundamental measurement in these radio occultation experiments is the Doppler shift of the received signal. When combined with a precise knowledge of the experiment geometry (obtained from concurrent observations of other GPS satellites), each sample of Doppler data can be converted to the

troposphere are certainly features to be exploited. One such example is the height of the marine boundary layer which should be identified with great accuracy³.

A key issue is how to retrieve refractive-index profiles in a horizontally non-uniform atmosphere. The simplest retrieval technique assumes there is no horizontal variation locally to the structure and therefore retrievals done in this manner will tend to smooth out the horizontal structure. **However**, each observation is an integral measurement across the whole atmosphere and therefore contains information on the horizontal structure. One improvement over the spherical symmetry assumption is to combine the occultation data with nadir viewing observations from other instruments and do retrievals on the combined data set. Because the high vertical resolution of the limb-sounding geometry complements the horizontal resolution of the nadir sounders, the two techniques **operating** in concert may be far more powerful than either alone. A somewhat analogous approach is to use information from models to provide an estimate of the horizontal variations which can then be used in the retrieval process. In addition if the radio occultations were to become sufficiently dense, the multiple occultation sounding.. in an area could be used to infer horizontal structure. The vertical to horizontal resolution ratio ($\sim 1:200$) is certainly appropriate for synoptic scale weather characterization. The degree to which the data can be applied to **mesoscale** weather phenomena is unclear at this point and will require detailed studies to reach some understanding in this area.

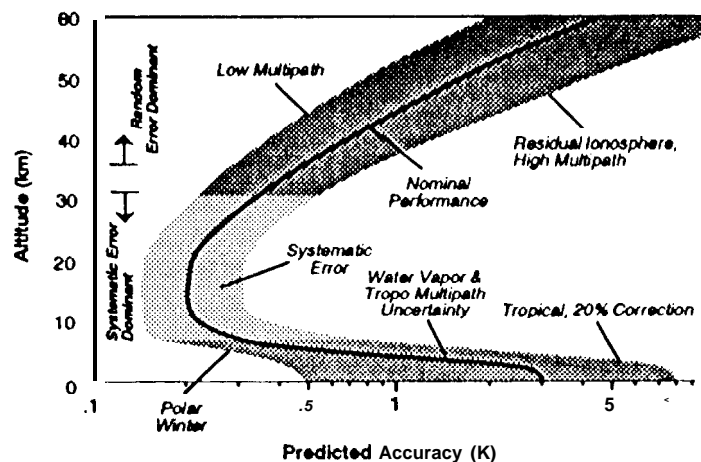


Figure 2 is a summary of the expected accuracy of the temperature retrievals as a function of altitude. The plot **breaks** down into three regions based on the dominant error source in each region. In the upper stratosphere random errors consisting of measurement errors and residual **ionospheric effects** dominate. **The** path length errors (excluding errors due to day time ionosphere) are of the order of 1 mm. The technique requires the use of the dual **GPS** frequencies in order to isolate and remove most of the ionospheric effect. **Higher** order ionospheric effects and bending can create a residual errors of 1-5 cm for

Figure 2: Predicted GPS atmospheric temperature accuracy occultations on the day side. This requires that ionospheric occultation measurement%

be taken and an electron density profile be obtained for every neutral atmospheric occultation in order to estimate the amount of error due to bending as well as higher order effects so it can be removed. In this way the ionospheric effect can be removed only to the extent that the ionospheric local spherical symmetry assumption is valid. Errors induced by the inaccuracy of the assumption will be estimated in a later study. Further analysis of the effect of the ionosphere and methods of removing it to do neutral occultation is needed in order to understand fully the accuracy of daytime stratospheric retrievals.

The region of greatest accuracy is the middle region covering the upper troposphere and lower stratosphere. This is labeled "systematic error" in **figure 2** and will probably be limited by knowledge of the horizontal variability of the refractivity. Absolute temperature error of less than a Kelvin is obtainable in altitudes between 10 and 45 km, and it can be as low as 0.1 K near the **tropopause**. The lower region is dominated by errors primarily related to the presence of water. These results are **based** on first principles and extrapolation of results from other planets. The capability to recover temperature structure with a precision of about 0,1 K has been demonstrated from occultation measurements of planetary atmospheres.

The technique and expected accuracy have been described by Kursinski et al.³. In the next section we describe all the components that constitute the total atmospheric refractivity and some of the basic assumptions that are used in going from refractivity to temperature. Then, some features of the technique such as the effect of scattering from water particles in the atmosphere are described (section 3). Section 4 examines the propagation of errors from one layer to the others, in addition, some general arguments regarding the effect of horizontal structure in the atmosphere on the retrieval is given. Section 5 is devoted to examining some of the limitation and usefulness of the technique in the troposphere.

2. SOURCES OF REFRACTIVITY

As μ , the index of refraction, is close to unity in the terrestrial atmosphere, it is convenient to define the refractivity $N = (\mu - 1) \times 10^6$. In the earth's atmosphere there are four sources of refractivity affecting the passage of the GPS signals. These are referred to as dry, moist, ionospheric and scattering terms respectively and the approximate equation for their dependence is as follows:

$$N = 77.6 \frac{P}{T} + 3.73 \times 10^5 \frac{P_w}{T^2} - 40.3 \times 10^6 \frac{n_e}{f^2} + 1.45 W \quad (1)$$

(dry term) (moist term) (ionospheric term) (scattering term)

where

- P = pressure in millibars,
- T = temperature in Kelvins,
- P_w = water vapor pressure in millibars,
- n_e = electron number density (m^{-3}),
- f = radio frequency in Hz,
- W = liquid water content in g/m^3

The dry term is due to the polarizability of molecules in the atmosphere, that is, the ability of an incident electric field to induce an electric field in the molecules. The moist term is due to the large permanent dipole moment of water vapor. The dry term dominates for altitudes between 0-90 km with the water vapor contribution becoming important in the lower troposphere. The ionospheric term is primarily due to free electrons in the ionosphere at altitudes higher than 90 km. The scattering term is due to water droplets suspended in the atmosphere and will be discussed later. As will be shown, the scattering term is small compared to the dry and moist terms.

The dispersive nature of the ionosphere causes the ionospheric refractivity term to depend on the frequency (3rd term in eq. (1)). This frequency dependence is exploited by the GPS dual frequencies so that the ionospheric term is isolated and removed to first order. After the removal of this term, higher order residual ionospheric terms will remain and will present a source of error in the stratosphere. This effect maybe particularly important on the day side. A careful examination of residual ionospheric effects and means of removing them will be the subject of an independent study. In the following discussion, ionospheric induced errors are ignored; however, some preliminary results on the effect of ionospheric bending are given elsewhere. Moreover, higher order ionospheric effects on the GPS signal for a ground user and means of reducing them can be found in the literature

In regions where the atmosphere is dry (above 10 km altitude) only the first term on the RHS of eq. (1) is significant. Combining this with the equation of state for dry air results in

$$\rho = 0.3484 \rho_0 \quad (2)$$

where p is the air density in kg m^{-3} . Comparing eqs. (1) and (2), it becomes evident that the density is directly proportional to refractivity for dry air. The pressure can then be obtained from the density by integrating the equation of hydrostatic equilibrium:

$$\frac{\partial P}{\partial h} = -g\rho \quad (3)$$

where h is height and g is the acceleration of gravity. Given p and P , eq. (2) can be used to obtain T .

However, the "moist term" can be substantial in the lowest scale height of the earth's atmosphere. This term also exhibits considerable variability with location and time. The separate contributions to N by the dry and the moist terms cannot be distinguished uniquely by the occultation measurements alone. The accuracy to which these terms can be separated is a function of climatic regime. We have taken a simple look at how well these can be separated in the two extreme climatic cases. As discussed by Kursinski et al.³, in tropical regions where the temperature structure is relatively constant, accurate estimates of water vapor profiles can be obtained using a simple average dry structure. In the other extreme, polar night, the moist contribution is so small that accurate temperature retrievals can be obtained down to the surface (see Fig. 5). This is consistent with the previously mentioned cold temperature retrieval capability complementing passive sensor observations. In spite of ambiguity in separating the dry and moist term in the troposphere, the total refractivity is still determined accurately in this region and can be used as an input parameter to weather and climate models.

3. PARTICLE SCATTERING

We return now to address the refractivity due to particle scattering. Scattering by particles suspended in the atmosphere will affect the propagation of electromagnetic signals. This effect was in fact exploited in the Voyager observations to recover the size distribution of the particles in the rings of Saturn⁷. Here we are concerned about the effects that water particles in the lower portions of the earth's atmosphere may have on the phase and amplitude of the occulted GPS signals. Water droplets are the primary source of scattering both because of their potentially large size and because of the large relative dielectric constant of water at microwave frequencies (~81). Because the GPS wavelengths are of order 20 cm, scattering by these particles falls into the Rayleigh regime.

To get an approximate answer we will assume spherical particles. Following the approach used by Gresh⁸ to interpret the Uranian ring occultation data, the extinction efficiency, Q (extinction cross-section divided by the geometric cross-section), under conditions of no absorption is

$$Q \text{ (no absorption)} \approx \frac{8(k\sigma)^4 (m^2 - 1)^2}{3(m^2 + 2)} \quad (4)$$

where $k = 2\pi/\lambda$, λ is the wavelength, σ is the particle radius and m is the index of refraction of the particle. Although water is somewhat lossy, the scattering extinction due to the real part of the index of refraction dominates the absorption effect. The less familiar, corresponding phase term is the phase-shift efficiency, P , which is defined analogous y to be

$$P \approx 2(k\sigma) \text{Re} \left(\frac{m^2 - 1}{m^2 + 2} \right) \quad (5)$$

These two terms represent the amplitude and phase shift of the scattered signal relative to the incident signal caused by a single scattering particle. A many particle thick model of scatterers results in

$$\frac{E_s}{E_i} = e^{-\tau/2} e^{i\phi_c} \quad (6)$$

where $\tau = \pi \sigma^2 n_p L Q$, $\phi_c = \pi \sigma^2 n_p L P$, E_i is the incident electric field, n_p is the particle number density and L is the thickness of the layer. The liquid water content, W , of the atmosphere is the particle number density times the volume per particle times the density of liquid water, ρ , integrated across all particle radii. For a monochromatic particle size distribution, the particle number density is proportional to the liquid water content divided by σ^3 . ϕ_c is proportional to $n_p \sigma^3$ and therefore is independent of particle size for a given W . From this it is easy to show that the refractivity due to scattering is

$$N = 1.5 \times 10^6 \frac{W}{\rho} \operatorname{Re} \left(\frac{m^2 - 1}{m^2 + 1} \right) \quad (7)$$

The refractivity due to scattering in eq.(1) is this same expression evaluated from $z = 81$. To evaluate the expressions of eqs. (4)-(7), the data from Atlas⁹ has been used to relate liquid water content to droplet particle diameter. For simplicity we have assumed all rain drops have the same radius. This is a reasonable first order assumption because the number densities fall off exponentially with drop radius and the distributions tend to be narrow⁹. The resulting changes in signal amplitude and phase are shown in Fig 3. The path length through the scattering particles is taken to be $L = 225$ km, which is the approximate horizontal path length through a layer having a vertical dimension of the first Fresnel zone. The amounts of liquid water used here are 2 and 5 gm/m^3 which are very large values; 2 gm/m^3 is actually the largest value for rain that is plotted in Figure 22 of Atlas⁹. Therefore, these results should be taken as upper bounds on the effect of atmospheric water droplets. The amplitude attenuation is negligible for particles less than 1 mm in radius which corresponds to the largest particle sizes typically observed.

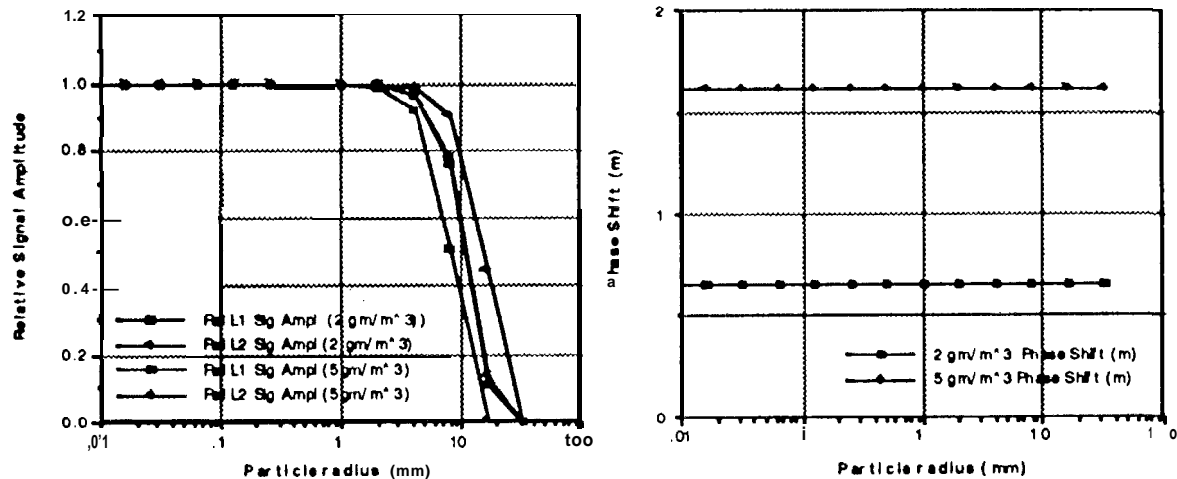


Fig. 3: Water droplet scattering effect on GPS signals (225 km path length)

The lack of dependence of the phase shift on particle radius for a fixed liquid water content is for the reason just cited. The phase shifts are of order 1 m or less. This is much larger than the sub-millimeter phase precision of the measurement system and would, by itself, be easily detectable in the

data. However, this will only occur in the lower troposphere where the delay due to the dry and moist terms is a few hundred meters and larger. Therefore, the scattering effect is at most a few tenths of a percent of the total refractivity effect and will be negligible. One can compare refractivity contributions in eq.(1) directly. For $W = 2 \text{ gm/m}^3$, the scattering refractivity will be approximately 3 in comparison to the dry and moist term combination which is approximately 300 near the surface indicating an approximate upper limit of 1% for the scattering contribution.

A radio occultation system operating at multiple wavelengths shorter than those of the present GPS system would have the potential to sense and discriminate between water droplet sizes and distributions. With sufficient rain along the path of an occultation, attenuation due to scattering will occur along with signal defocusing due to bending. The refractivity structure retrieved from the phase data allows the attenuation due to defocusing to be estimated and removed from the observed attenuation. Any residual signal decrease would be extinction due to scattering. The same approach has been applied to occultation data taken at the outer planets to estimate the ammonia vapor density. The amount of attenuation would be a function of wavelength and the attenuation difference between wavelengths could be used to determine the size of the raindrops much in the manner in which the ring particle distributions were determined for Saturn's rings.

4. SIMULATION SYSTEM

We have created a system which generates simulated occultation data by ray-tracing and then processes the data in a realistic manner. Our simulation system allows us to study different sources of error which might include measurement noise, ionospherically induced error, and errors due to assuming the wrong shape of contours of constant refractivity. In a previous work, we have shown in some detail the effect of measurement noise⁵. In this section, an intuitive approach to understand how a refractivity error in one layer propagates into other layers is given. We also give some general approach to understand the effect of the presence of horizontal structure in the atmosphere on the retrieval process.

4.1 Impulse response

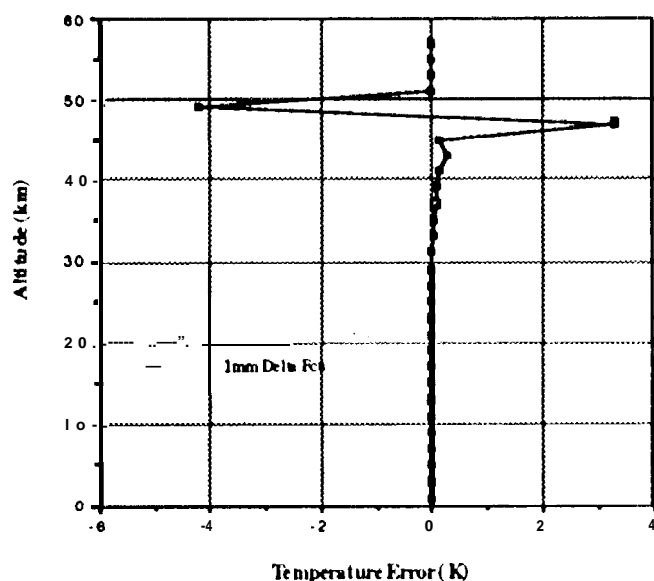


Fig 4: Effect of individual measurement error on inversion technique

This is accomplished using the estimated refractivity of the first shell derived from the first

A useful starting point is the impulse response of the system, that is, how does the inversion system respond to an error in a single measurement. To do this we generate a set of measurements covering one occultation limb-scan and add a noise spike to a single measurement and then invert this data set with the one modified point. The result is shown in Fig. 4 and indicates primarily a double pulse error response. This can most easily be understood in terms of the onion shell analogy where each additional measurement is used to peel away the overlying shells and isolate the contribution of the next deeper shell of the atmosphere. Beginning at the top of the atmosphere, the raypath of the first delay measurement propagates through the outermost atmospheric shell. The next raypath of the next measurement passes through the two outermost shells. To estimate the contribution of the second shell, the amount of delay due to the outermost or first shell must be subtracted off.

measurement. This scenario continues on down through the atmosphere with the refractivity estimate for each layer depending on the measurements made above it.

Returning to the noise spike, suppose we have n measurements beginning at the top of the atmosphere and ending at the surface with the i^{th} measurement containing the noise spike. The higher $i-1$ altitude retrievals derived from measurements made before the spike occurs are unaffected by the spike. The temperature of the i^{th} shell associated with the measurement which includes the noise spike is in error. This is the upper of the two larger pulses in Fig. 4. The temperature of the $i+1$ layer immediately below the noise spike layer is also in error because the estimated contribution of the overlying i^{th} layer is incorrect. If the noise spike were positive, that is, the observed delay were too large, then the estimated refractivity of the i^{th} shell would be larger than the true refractivity in that shell. Because the i^{th} shell refractivity has been overestimated, its contribution to the $i+1$ measurement will be overestimated causing the contribution of the $i+1$ layer refractivity to be underestimated. Therefore the error of the retrieved $i+1$ layer refractivity will have the opposite sign of that of the i^{th} layer. The power of this technique is that the retrieval error is basically limited to these two layers because, in retrieving the next lower layer, the $i+2$ layer, the contribution of the errors in the i and $i+1$ layers almost cancel resulting in very little error in this layer and all the subsequent layers as is apparent in Fig. 4. So to a good approximation the effect of errors due to individual measurements or layers is confined to the layer associated with the measurement and the layer immediately below it.

4.2 Errors in shape

A potentially important source of error in these retrievals is the shape of the refractivity structure. To gain understanding here, we will again use the onion skin analogy. The atmospheric Doppler measurements are integral measurements, that is, each measurement is an integral of the quantity of interest, namely the refractivity structure. Inverting these measurements to recover the refractivity requires knowledge of the shape of the contours of constant refractivity. An important source of error in these retrievals is incorrect shape of these contours. To gain insight into this effect, we consider the stratospheric case where bending is small and the atmospheric delay is dominated by the slowing of the signal velocity. The atmosphere can be thought of as a series of concentric shells each with a constant refractivity. The atmospheric delay caused by the passage of the signal through a single shell is simply:

$$\delta_i = (\mu_i - 1) \lambda_i / c \quad (8)$$

where μ_i is the index of refraction in the i^{th} layer, A_i is the path length of the portion of the ray within the layer, c is the speed of light in a vacuum and i denotes the layer number. The total delay due to the atmosphere is the sum of the delays of the individual layers. Recovering the index of refraction from observations of delay requires that the λ_i 's be known. An error in the assumed shape will cause the values of λ_i 's to be incorrect, leading to errors in μ_i .

The obvious point of symmetry along the raypath is the point where the ray reaches its minimum altitude with respect to the earth. This is approximately the midpoint of the raypath within the atmosphere. Relative to this point, the shape error can be expanded in terms of some set of even (symmetric) and odd (antisymmetric) functions such as sine's and cosine's or polynomials. For odd or antisymmetric terms, the path length within the shell is larger than the model shape on one side of the raypath midpoint but smaller by the same amount on the other side. Therefore the net effect on the refractivity retrieval of these terms is to first order zero and only the even terms of the shape error contribute to errors in refractivity. To get a first order estimate of the magnitude of this effect, we will consider the simplest even shape error, a quadratic function.

To accomplish this we will use polar coordinates where the origin is at the center of the earth (or the center of curvature of the refractivity contours) and θ is the angle orthogonal to the radial direction measured from the occultation midpoint. At a constant radial distance, r , the quadratic dependence of N is $N(r, \theta) = N(r) (1 + a \theta^2)$ where a is a constant scale factor. This produces a fractional error in the ray path length within a shell of approximately $2aH/r_0$, where H is the local refractivity (and therefore density) scale height and r_0 is the radial length from the center of the earth to the raypath at the occultation midpoint. The assumed path length in the shell will underestimate the actual path length resulting in an overestimate of the refractivity within the shell by this same fractional amount. Now what is a representative value for a ? A simple case is the refractivity gradient associated with the horizontal transition from midlatitudes to the very cold polar region during winter. A typical case at 10 mb over the winter pole given in Figure 3.6 of Brasseur indicates a is on the order of 0.3 rad^{-2} under these conditions ¹⁰. H is on the order of 6.5 km and r_0 is approximately 6420 km resulting in a fractional refractivity (and therefore density) error of 7×10^{-4} .

Under the assumption that there is no pressure error, fractional density error would be the same as fractional temperature error (as can be seen from eq. 2) which translates to 0.15 K of temperature error for the example considered above. However, pressure is estimated by integrating the vertical density via the hydrostatic equilibrium equation; therefore, pressure error will tend to follow density error. Consider the end-member case where this fractional shape error is constant with altitude. This will cause the density to be in error by this same fractional amount at all altitudes. Because pressure is the integral of the density and density is everywhere in error by a constant fractional amount, the pressure will also be in error by this same fractional amount over all altitudes. The net effect on temperature will be zero because in taking the ratio of pressure to density, their identical fraction errors will cancel resulting in zero temperature error. The opposite extreme occurs when the fractional density error changes rapidly with altitude. Under these conditions, the fractional temperature error will be close to that of the density. Rapidly here means relative to a scale height. Because the atmospheric density structure is exponential, most of the contribution to the pressure integral occurs over the two scale heights immediately above the height at which the pressure is being evaluated. Therefore errors in density which change rapidly relative to a scale height will map rather directly into temperature errors whereas slowly varying density errors will produce relatively little temperature error.

A final comment in this area concerns knowledge of the shape of the constant refractivity contour. In the example given above, the shape of the constant density contours associated with polar night was treated as spherical. Of course this would not be the case and the real inversions would take the best knowledge of the shape into account. The general point is that if a structure in the atmosphere can be characterized through direct observations or modeling, then the inversion of the occultation measurements would account for the structure and the accuracy of the retrievals would be improved.

5. TROPOSPHERIC RETRIEVALS

The GPS occultations represent a somewhat unique opportunity to routinely probe the troposphere in a limb sounding geometry. Because aerosols and clouds particles present in the troposphere cause signal extinction, routine limb sounding at these altitudes must be done at relatively long wavelengths. However, achieving -1 km vertical resolution with a passive sensor requires an aperture which is a few thousand wavelengths in diameter. As already mentioned, the resolution of the occultation technique is limited by Fresnel diffraction rather than aperture diffraction resulting in ~1 km vertical resolution at 20 cm wavelengths. The strength of this technique in the troposphere will be its vertical resolution which will range from -1 km down to 100 meters where the refractivity vertical gradients are large³. In fact under conditions where the horizontal gradients are small the vertical resolution can be pushed beyond the Fresnel diffraction limit by sampling and subsequently inverting the diffraction pattern in a manner which is essentially holography. This is a capability presently unique to the radio occultation observations and is possible because the signals are monochromatic and therefore have a well defined phase. The same concept was applied to retrieving the opacity structure

of the **Uranian** rings improving the **Fresnel** diffraction limited resolution by more than an order of magnitude. The first routine application of this capability to planetary atmospheres will commence. at the end of this year with the pressure and temperature profiles of the Martian atmosphere generated by the Mars Observer radio occultations¹¹.

Water vapor can have a large effect on the microwave refractivity of the lower portion of the earth's atmosphere. Because of the importance of water vapor in weather and climate, we have begun to explore how the GPS occultation signals might be utilized in this regard. A number of inquiries have been made concerning the possibility of using GPS occultations to recover water vapor densities in the upper troposphere and stratosphere. However, at these altitudes the water vapor refractivity signature is too small relative to the dry refractivity term to be useful. The small amount of water vapor present at these altitudes slightly increases the apparent **density** of the dry gas needed to account for the retrieved refractivity structure. This becomes a small source of error on the retrieved temperature profiles in these regimes.

In the troposphere, there are two major issues concerning what can be accomplished with these observations. The first is how accurately can refractivity be retrieved in the presence of relatively large horizontal variations in the refractivity structure. The techniques to retrieve the refractive-index profile in an atmosphere which varies horizontally have been developed and the results will be presented in a future paper. The second issue is how well can the moist and dry terms of the refractivity be separated and further interpreted. To answer the latter question a series of simulations have been carried out using a special set of global temperature and moisture profiles which were prepared as part of a large effort for atmospheric retrievals from satellite-based passive radiometers. The profiles are known as the **TIROS** Initial Guess Retrieval (**TIGR**) data and consist of 1761 radiosondes that have been carefully selected, screened, and quality-controlled by scientists within the **Laboratoire de Météorologie Dynamique** in France.

Since both temperature and moisture contribute to the refractive index in the lower troposphere, in general one can not uniquely solve for either one without knowledge of the other. However, there are some situations, such as during polar winter, or in the tropics, where moisture or temperature can be retrieved in the lower troposphere by applying some valid assumptions. In order to estimate how well one can separate the dry and wet terms in these regions a selected set of the TIGR radiosonde data is used as follow: From the temperature, humidity and pressure measurements of a particular TIGR radiosonde data, the vertical refractivity profile can be computed, The computed refractive index is then modified by adding a white Gaussian noise value having a mean of zero and a standard deviation that varies with height, The standard deviation was assumed to be 50% of the refractivity at 70 km and decreased exponentially to 0,005% of refractivity near the surface; these values are consistent with a measurement error of about 0.1 cm in path delay near 70 km and 1 cm near the surface. The noise-modified refractivity profile is used as the measurement from which attempts are made to recover either temperature or moisture.

The result of a retrieval for a cold polar profile is shown in Figure 5. The surface temperature for this sounding is cold at 248 K and the dew point is about 4 K lower than the temperature up to about 8 km, Although the air has a low water content, it helps to assume that it is not completely dry. Consequently, a relative humidity of 50% was used to represent the air below 7.5 km. From eq. (1), it can be seen that a temperature also has to be assumed in order to compute the contribution of moisture to the total refractive index. For the sole purpose of estimating the contribution of moisture to the refractivity, a mean lapse rate of temperature of 6 K km⁻¹ was used from 7.5 km down to the surface. The temperature from 70 km down to 7.5 km was retrieved through the process described by Eqs. (1)-(3). Below 7.5 km, the estimated moisture term of the refractivity was subtracted from the noise-modified refractivity profile in order to get the temperature or density contribution.

Then the temperature could be retrieved using the same process as for dry air. The resulting temperature error is within 0.7 K, and for much of the sounding the error is less than 0,3 K. This is

typical of the type of temperature retrieval that is possible when the temperature near the surface or at any other level is colder than about 250 K. When the surface temperature approaches 270 K, then the unknown contribution of the moisture increases the error in the retrieved temperature profile.

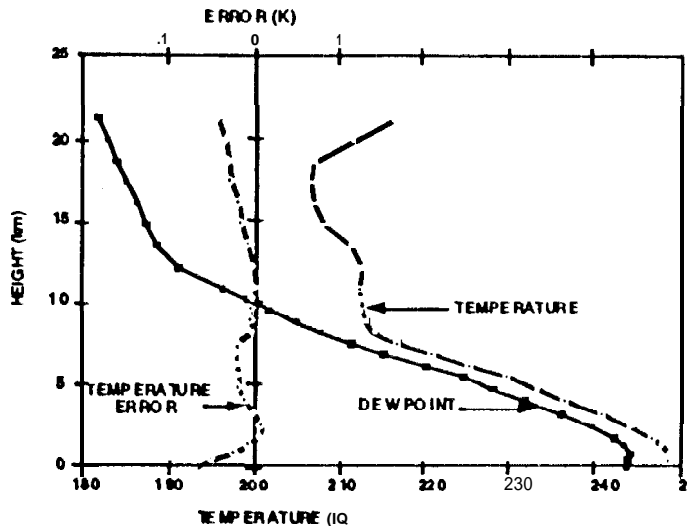


Fig. 5: Temperature error for TIGR polar-2 sounding #1201

A different situation occurs in tropical regions where temperatures tend to have less annual variability but moisture contributes significantly to the refractivity. In these regions, the approach is to retrieve temperature down to some level where moisture starts introducing unacceptable errors. Below such a level, procedures are introduced to estimate the temperature profile down to the surface. Then the contribution of temperature to the refractivity is computed and subtracted from the noise-modified profile of refractivity. The

remainder is the contribution by the moist term, and consequently the moisture profile can be estimated,

6. CONCLUSION

We have attempted to provide some insight into the mechanism of the radio occultation technique and its potential performance in the areas of temperature and moisture retrievals in the earth's atmosphere. We have discussed the effect of scattering due to water droplets which has not as yet been discussed with regard to this technique and provided a simple derivation for the refractivity term it creates and an approximate upper bound to its magnitude. We have also provided some insight into the effect of horizontal structure on the retrieval process. This is particularly important because it is probably the largest error source in the tropopause region where this technique may provide sub-kelvin temperature retrievals. The example of a large scale structure due to radiative cooling above the winter pole resulted in an error of 0.15 K whose small size is very promising. Further work is being done to produce an error probability distribution due to horizontal structure based on realistic models in the lower and middle atmosphere. One other important issue to be addressed is the removal of the daytime residual ionospheric effects for stratospheric soundings. The radio occultation technique is an old and established method in planetary remote sensing. Utilizing this technique with the GPS satellites has a number of unique features that complement and enhance other passive sounding based methods,

Acknowledgment: Part of this work was carried out at the Jet Propulsion Laboratory, California institute of Technology, under the National Aeronautics and Space Administration.

7. REFERENCES

- [1] G. Fjeldbo, A. J. Kliore, and V. R. Eshleman, "The neutral atmosphere of Venus as studied with the Mariner V radio occultation experiments", *Astronom. J.*, vol. 76, No. 2, pp. 123-140, March 1971.